Constraints on dark matter-nucleon effective couplings in the presence of kinematically distinct halo substructures using the DEAP-3600 detector

Ariel Zuñiga Reyes
Institute of Physics, National Autonomous University of Mexico (UNAM)

14th International Conference on Interconnections between Particle Physics and Cosmology (PPC2021), 20 May 2021. University of Oklahoma.

The DEAP-3600 experiment

DEAP-3600
(Cube Hall)

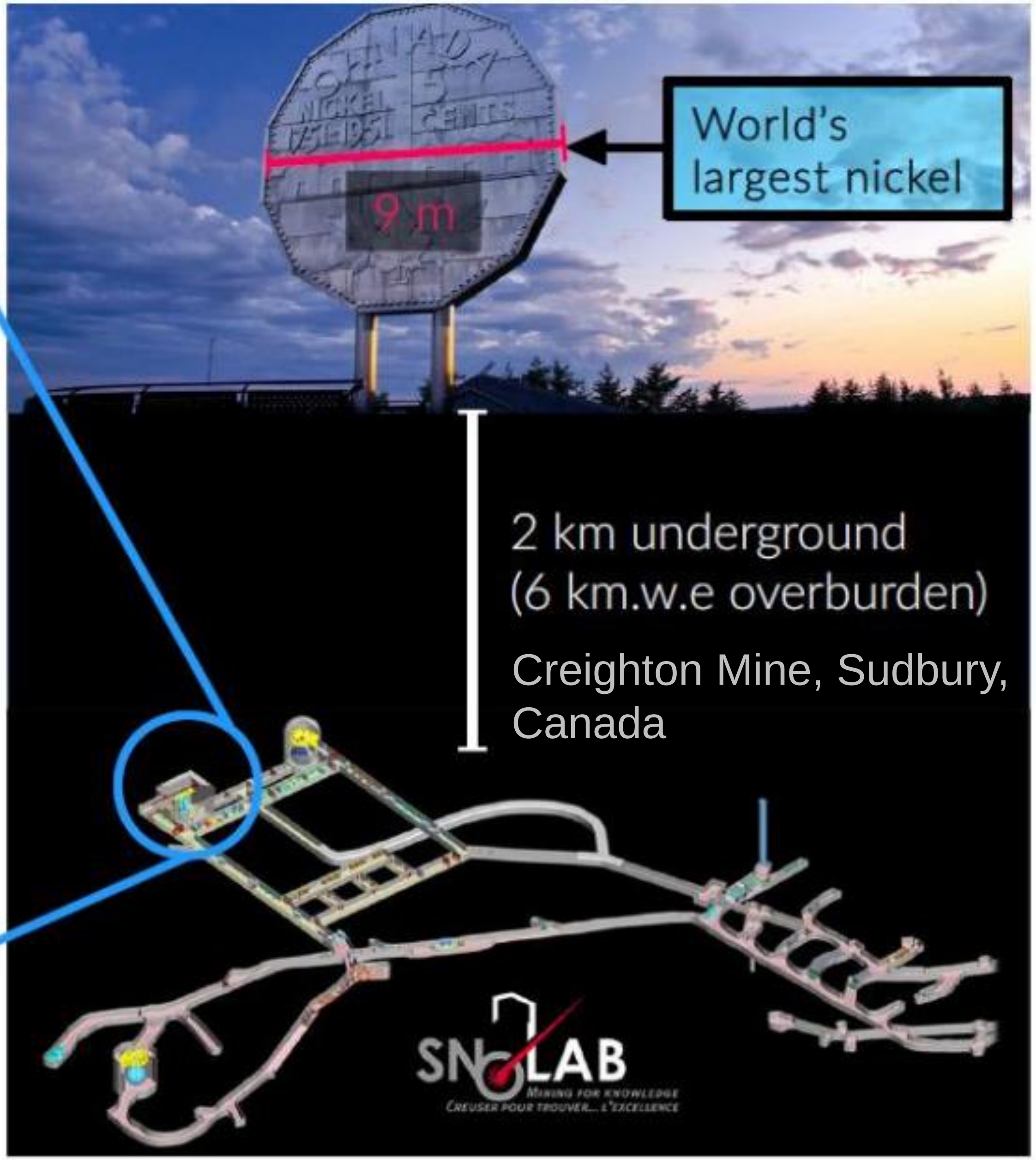

Dark Matter Experiment using Argon Pulse-shape Discrimination (DEAP)

- ~3.3 tonnes single-phase liquid argon (LAr) target inside a spherical, radiopure acrylic vessel.
- Optimized for collecting scintillation light due to WIMP-induced nuclear recoils after scattering with ^{40}Ar nuclei. Electron recoils (background) are rejected with the Pulse-Shape Discrimination approach.
- A TPB (tetraphenyl butadiene) layer shifts 128 nm VUV scintillation to visible.
- Acrylic light guides transport wavelength-shifted photons to 255 Hamamatsu R5912 HQE 8" PMTs.
- Foam filler blocks between light guides provide further insulation and shielding.
- The whole setup is immersed in a water tank (passive shield for outside γ-rays and neutrons).
- Outward looking PMTs work as a muon Cherenkov veto.

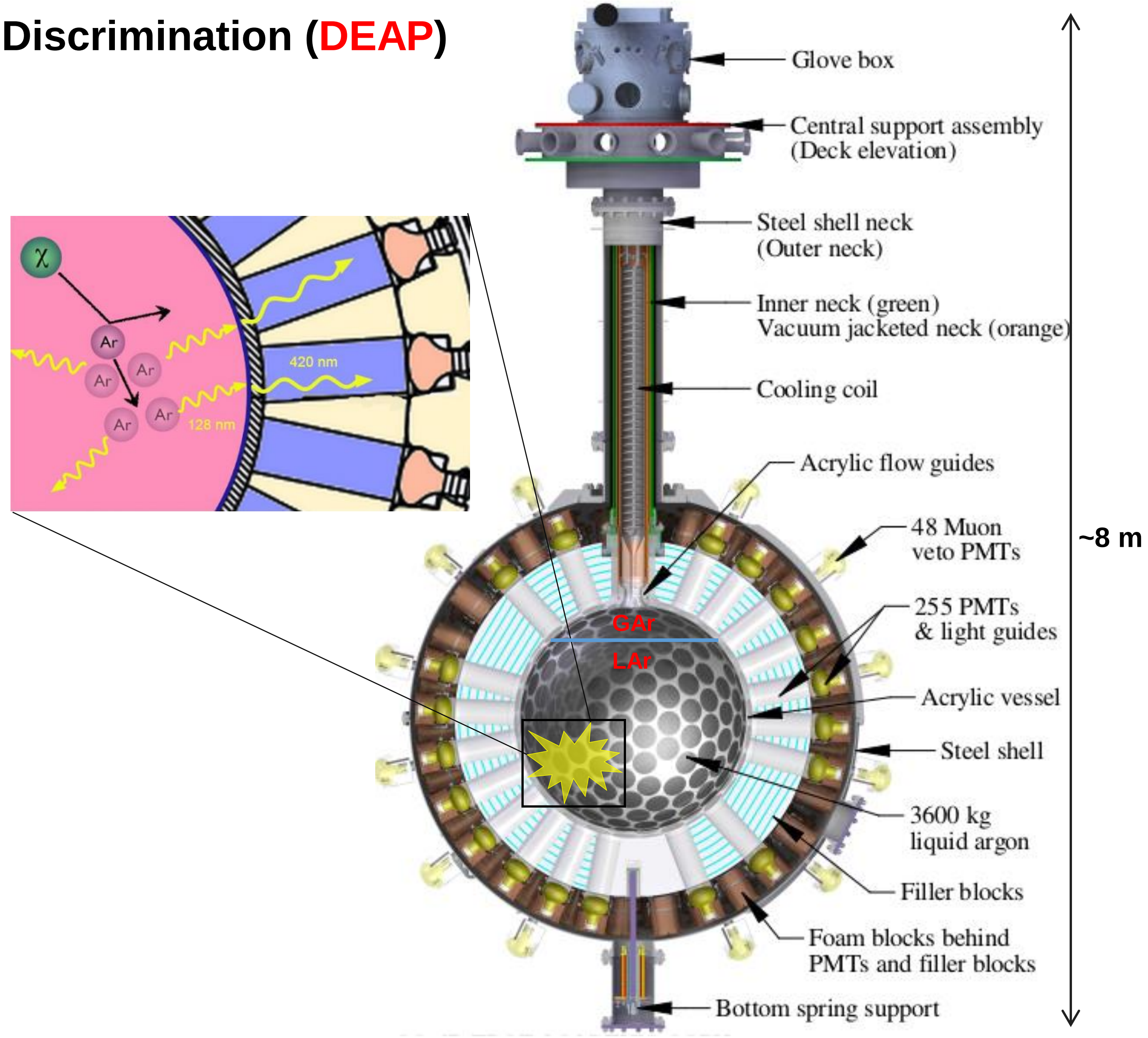

Astropart. Phys. 108, 1 (2019)

DEAP-3600 results: 2^{nd} WIMP search campaign

Phys. Rev. D 100, 022004 (2019)
- 231 live-days (first year of operation)
- 3279 kg of liquid argon (LAr)
- 758 tonne·days exposure

- After all cuts, no WIMP-like signals.
- Detailed description of backgrounds.
- Demonstration of the Pulse-Shape Discrimination (PSD) power.

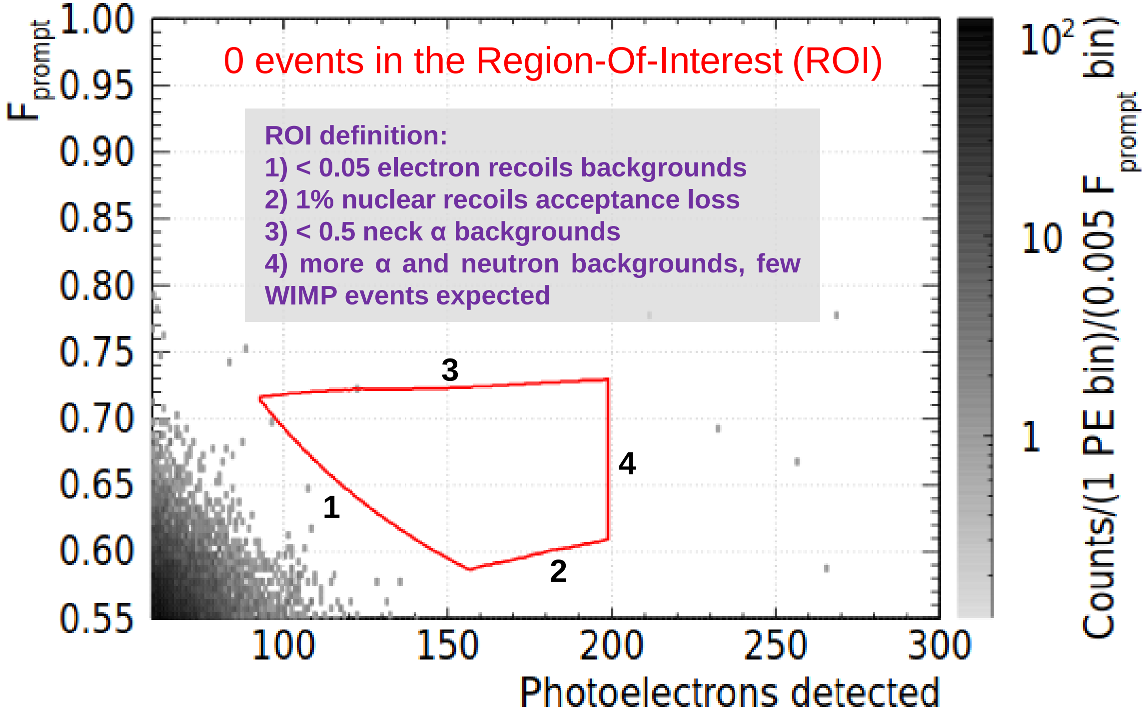

Most sensitive limit with a LAr target!

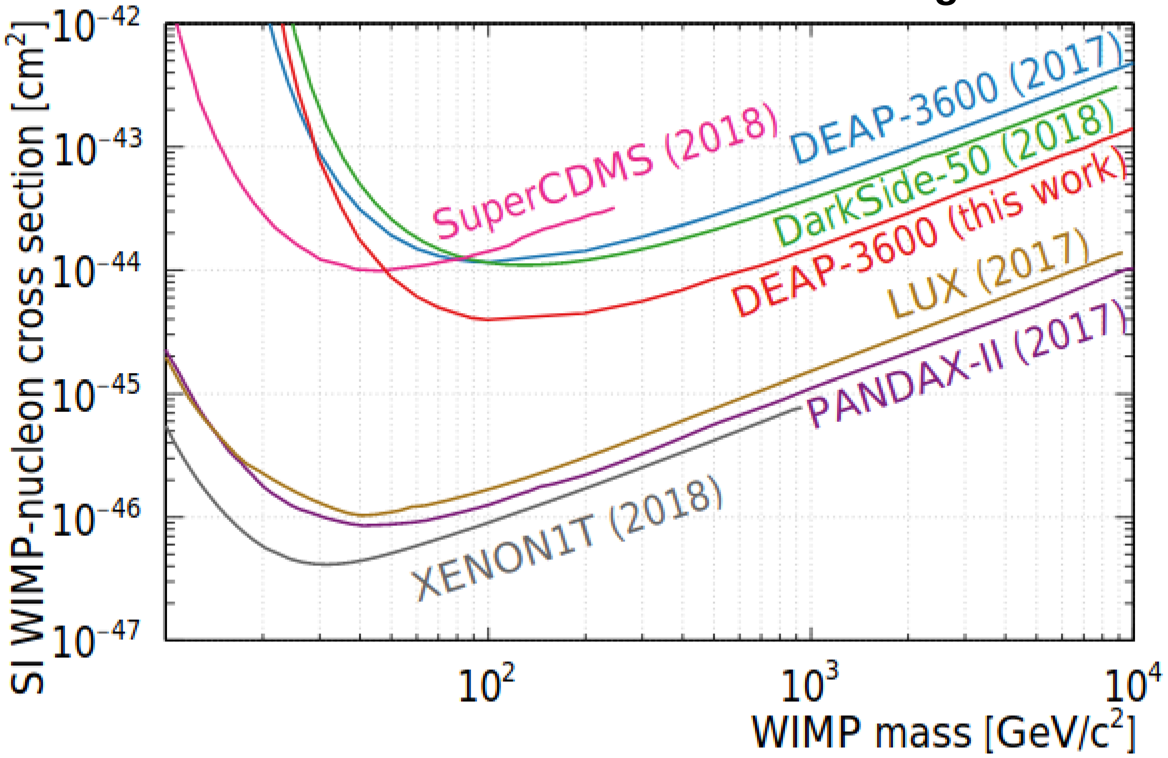

Setting direct-detection limits

Exclusion curves typically determined by direct detection experiments based on standard assumptions for astrophysics and particle physics models:

- Allows for direct comparison between different experiments

- Not necessarily an accurate description of the local DM distribution/nuclear coupling

Important features in exclusion curves can be missed or the parameter space may be overly constrained.

Effective operators for [40] Ar

$$\mathcal{O}_1 = 1_\chi 1_N,$$

$$\mathcal{O}_3 = i\vec{S}_N \cdot \left(\frac{\vec{q}}{m_N} \times \vec{v}_\perp\right),$$

$$\mathcal{O}_5 = i\vec{S}_\chi \cdot \left(\frac{\vec{q}}{m_N} \times \vec{v}_\perp\right),$$

$$\mathcal{O}_8 = \vec{S}_\chi \cdot \vec{v}_\perp,$$

$$\mathcal{O}_{11} = i\vec{S}_\chi \cdot \frac{\vec{q}}{m_N},$$

$$\cancel{\mathcal{O}_{12} = \vec{v}_\perp \cdot (\vec{S}_\chi \times \vec{S}_N),}$$

$$\cancel{\mathcal{O}_{15} = -\left(\vec{S}_\chi \cdot \frac{\vec{q}}{m_N}\right)\left[(\vec{S}_N \times \vec{v}_\perp) \cdot \frac{\vec{q}}{m_N}\right].}$$

Building block:
S_χ : DM spin, **S_N** : nucleon spin, **q** : momentum transfer and **$v^\perp$** : component of the velocity perpendicular to q.

Non-Relativistic Effective Field Theory (NREFT): provides a general formulation for possible dark matter-nucleus interactions and a better description of the nuclear response.

JCAP 11 (2010) 042, JCAP 02 (2013) 004, Phys. Rev. C 89, 065501 (2014)

Interaction Lagrangian (L_{int}): a sum over i effective operators, where c_i is the coupling constant associated with the O_i operator.

$$\mathcal{L}_{\text{int}} = \sum_i c_i \mathcal{O}_i$$

Photon-mediated interactions can also be parametrized as linear combination of NREFT operators:

Anapole

$$\mathcal{O}_{\mathcal{A}} = c_{\mathcal{A}} \sum_{N=n,p} (Q_N \mathcal{O}_8 + g_N \mathcal{O}_9)$$

Millicharge

$$\mathcal{O}_{\mathcal{M}} = e^2\, \epsilon_\chi \frac{\mathcal{O}_1}{q^2}$$

Electric dipole

$$\mathcal{O}_{\mathcal{ED}} = 2\, e\, d_\chi \frac{\mathcal{O}_{11}}{q^2}$$

Magnetic dipole

$$\mathcal{O}_{\mathcal{MD}} = 2\, e\, \mu_\chi \sum_{N=n,p} \left[Q_N\, m_N \mathcal{O}_1 + 4\, Q_N \frac{m_\chi m_N}{q^2} \mathcal{O}_5 + 2\, g_N\, m_\chi \left(\mathcal{O}_4 - \frac{1}{q^2}\mathcal{O}_6\right)\right]$$

Astrophysics model: Non-standard DM halo substructures in Gaia & SDSS data

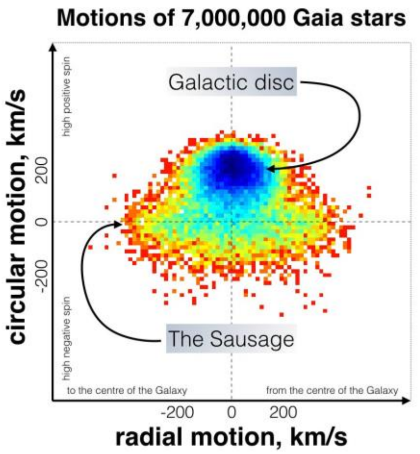

MNRAS 478:1(2018), p.611–619

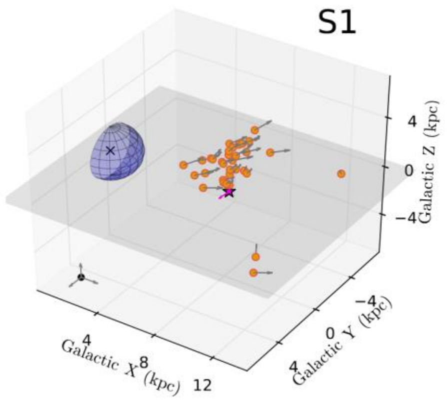

Phys. Rev. D 98, 103006 (2018)

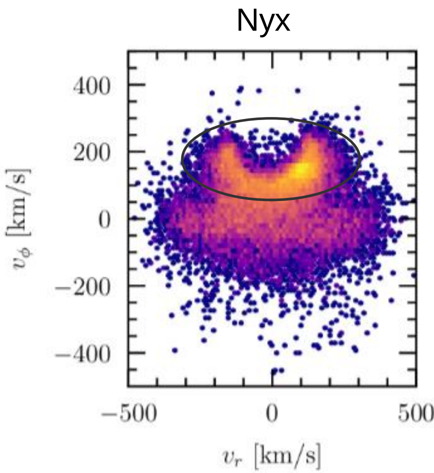

Nat. Astron. Vol. 4, p.1078-1083 (2020)

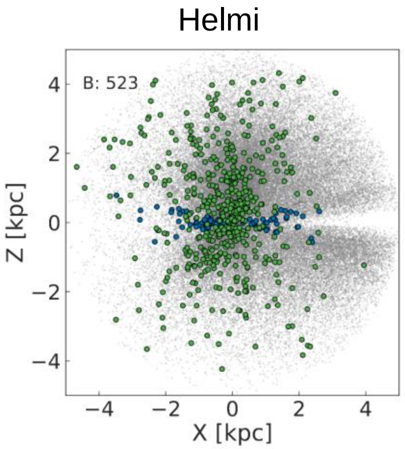

Astrophys. 625, A5 (2019)

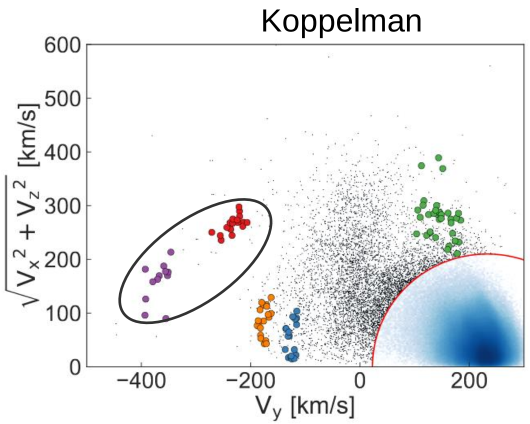

Astrophys. J. 860, L11 (2018)

Gaia Sausage: Debris flow with high radial velocity, likely caused by a merger event with a dwarf galaxy.

S1: Retrograde stellar stream; member stars impact almost head-on the Solar System (v ~ 500 km/s). a.k.a. DM hurricane.

Nyx: Prograde stellar stream; evidence suggests stream intersects solar neighbourhood

Helmi: stellar stream in the solar neighbourhood in several galactic surveys; could indicate similar substructure in the local DM halo

Koppelman 1 & 2: pair of stellar streams in solar neighbourhood; appear to be recently accreted

Simulations suggest that these stellar populations can be used as tracers for DM, though there may be significant uncertainty for streams [Necib (2019) ApJ 883 27, Necib (2019) ApJ. 874, 3].

Considered a generic model of “in-falling clumps” (IC) to describe extra-galactic DM accreted into the Milky Way.

WIMP-nucleus scattering theory

Differential event rate

$$\frac{\mathrm{d}R(t)}{\mathrm{d}E_r} = N_T \frac{\rho_0}{m_\chi} \int_{v>v_{\min}} v \, \boxed{f(\mathbf{v}+\mathbf{v}_\mathrm{E}(t))} \, \boxed{\frac{d\sigma_T(v,E_r)}{dE_r}} \, \mathrm{d}^3 v$$

<u>Velocity Distribution Function</u>
(astrophysics model)

Maxwell-Boltzmann distribution

$$f(\mathbf{v}) = \frac{1}{\sqrt{2\pi}\sigma} \exp\left(-\frac{|\mathbf{v}|^2}{2\sigma^2}\right)$$

DM velocity distribution with the substructure

$$\boxed{f_\mathrm{DM}(\vec{v}) = (1-\eta_\chi)\, f_\mathrm{R}(\vec{v}) + \eta_\chi\, f_\mathrm{Sub}(\vec{v})}$$

f_R: velocity distribution of a nearly round dark halo - SHM (Maxwell-Boltzmann distribution).

f_{Sub}: velocity distribution of the substructure (3D Gaussian distribution).

$\boldsymbol{\eta_\chi}$: relative DM density in substructure (0-30% for streams and ICs, 0-70% for Gaia Sausage).

<u>Differential cross-section</u>
(particle/nuclear physics model)

Spin-independent cross-section

$$\frac{d\sigma_T(v,E_r)}{dE_r} = \frac{m_N A^2 \sigma_p^{\mathrm{SI}}}{2\mu_p^2\, v^2} F^2(E_r)$$

NREFT cross-section

$$\boxed{\frac{d\sigma_T(v,E_r)}{dE_r} = \frac{4\pi}{2J+1} \sum_k \sum_{\tau=0,1} \sum_{\tau'=0,1} R_k^{\tau\tau'}\left[v_T^{\perp 2}, \frac{q^2}{m_N^2}, \left(c_i^\tau\, c_j^{\tau'}\right)\right] W_k^{\tau\tau'}(y).}$$

R: DM response function (contains the couplings strength)
W: nuclear response function (depends on the target used)
k-index: represents 6 interactions (M, Φ", Φ"M are the non-zero for ^{40}Ar).

- ✓ M = describes the nucleon density inside the nucleus.
- ✓ Φ" = related to the angular momentum and spin of nuclei. It favors heavier elements with large, not fully occupied, orbitals.
- ✓ Φ"M = interference term, product of Φ" and M.

Velocity distributions modeled

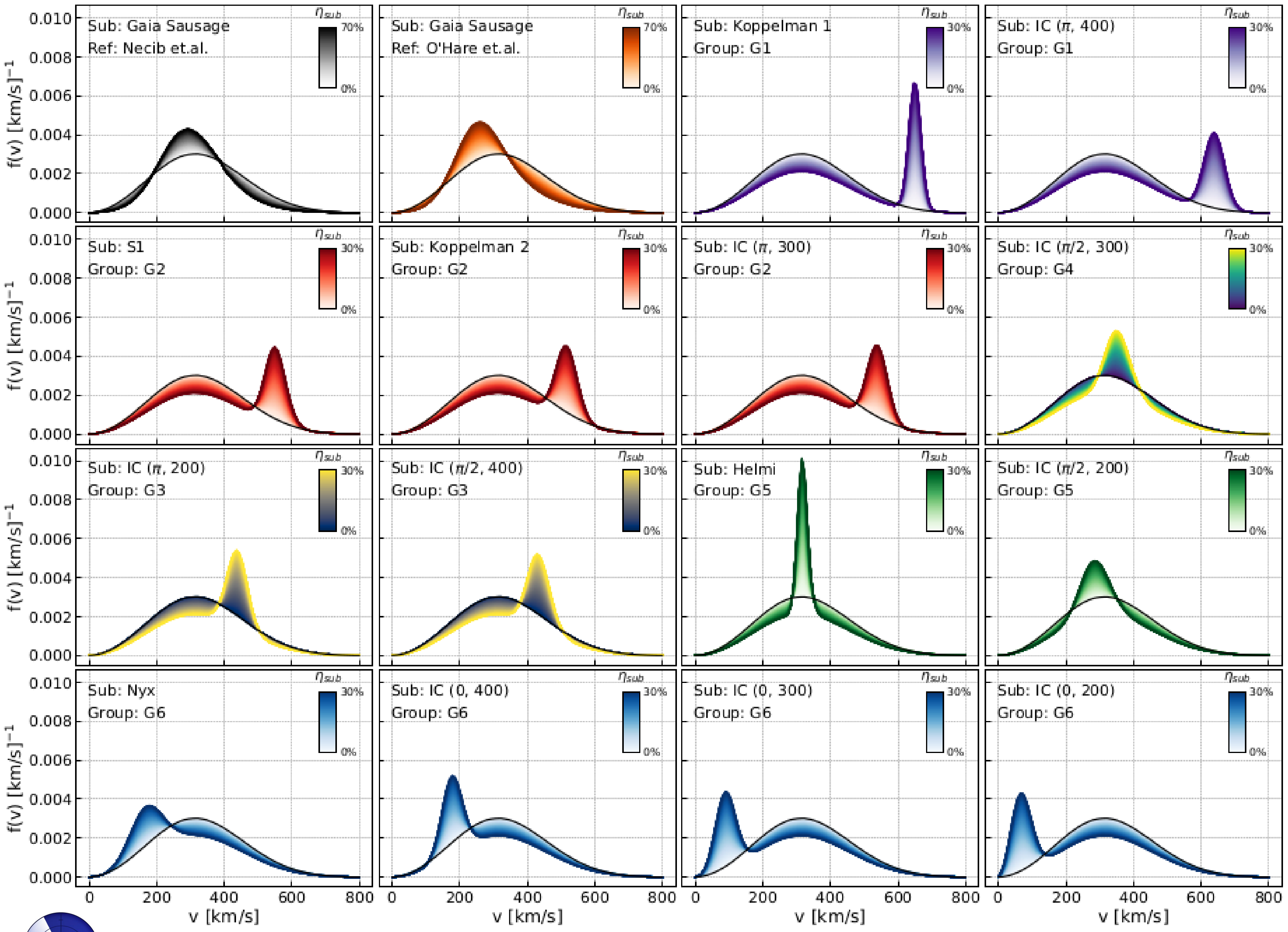

Color gradient: indicates the relative DM density in each substructure.

- Streams & ICs: 0 % (light) to 30 % (dark).
- Gaia Sausage models: up to 70 %.

The solid black line corresponds to the SHM.

The distributions are normalized to 1 and boosted to the Earth reference frame.

Arranged in groups from G1-G6.

(G1, G2, G3) - Fast
(G4, G5) - Medium speed
(G6) - Slow

The first velocity distribution in each group was used.

Phys.Rev.D 102 (2020) 8, 082001

Recoil energy spectra

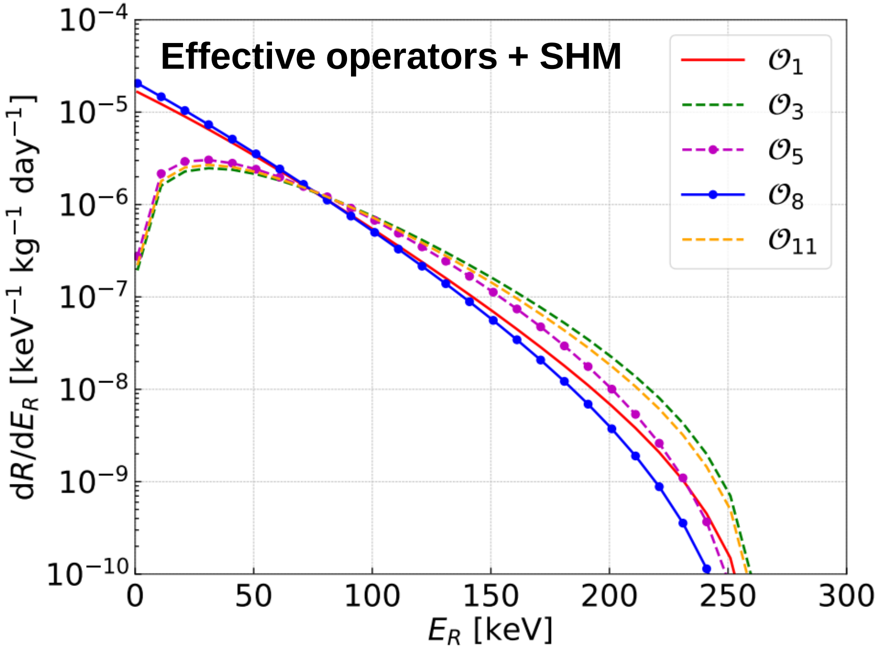

Phys.Rev.D 102 (2020) 8, 082001

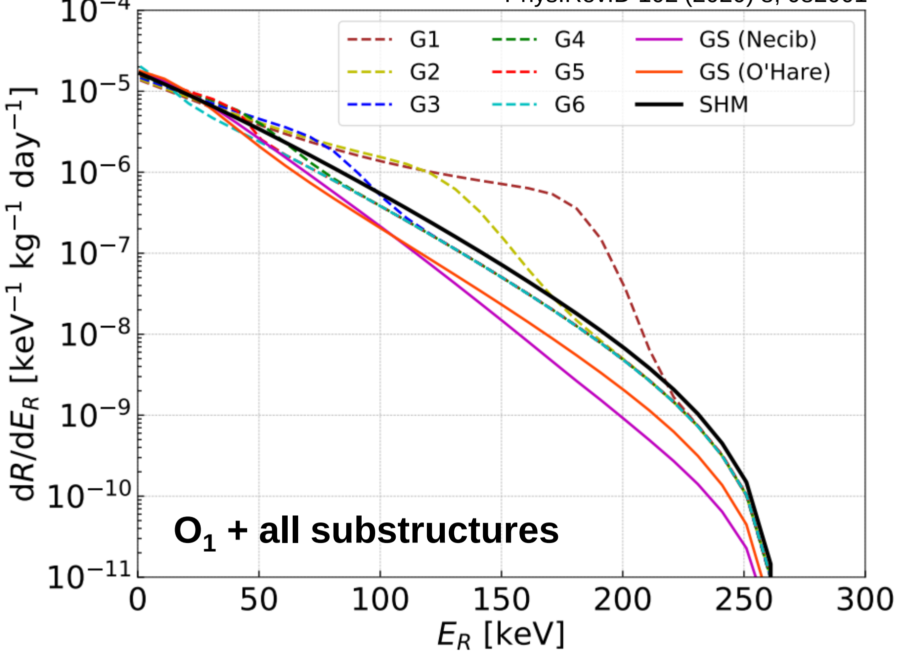

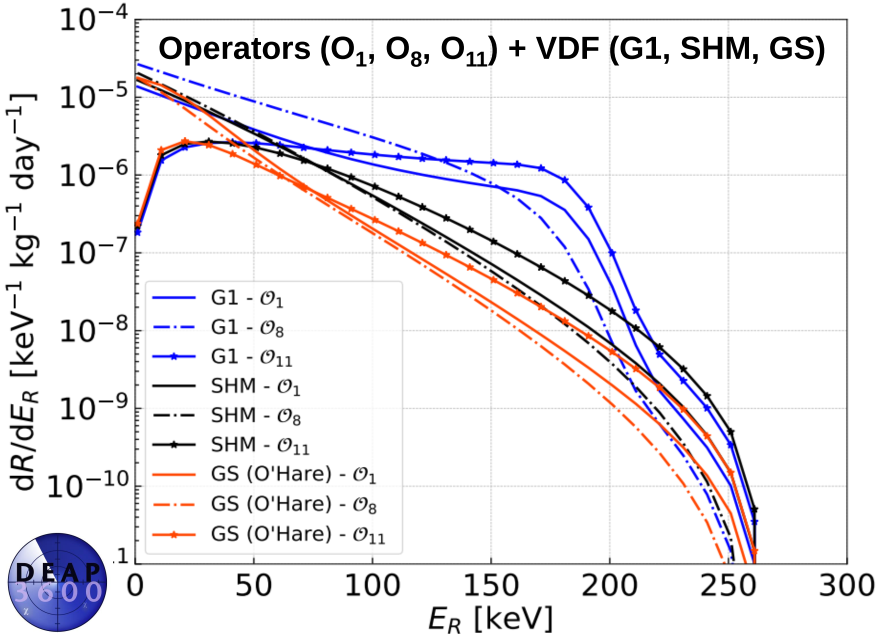

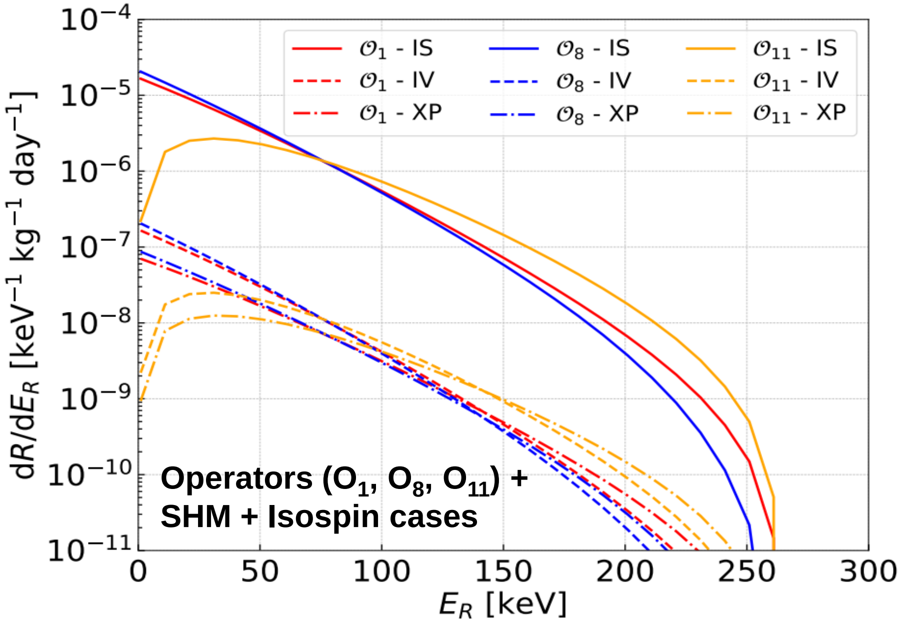

All curves drawn for m_χ = 100 GeV/c^2

O_1 ~ 1 , uses M

O_3 ~ q^2 , uses Φ”

O_5 ~ $(v_\perp q)^2$, uses M

O_8 ~ $v_\perp{}^2$, uses M

O_{11} ~ q^2 , uses M

Constraints for effective operators + isospin-violating scenarios

Phys.Rev.D 102 (2020) 8, 082001

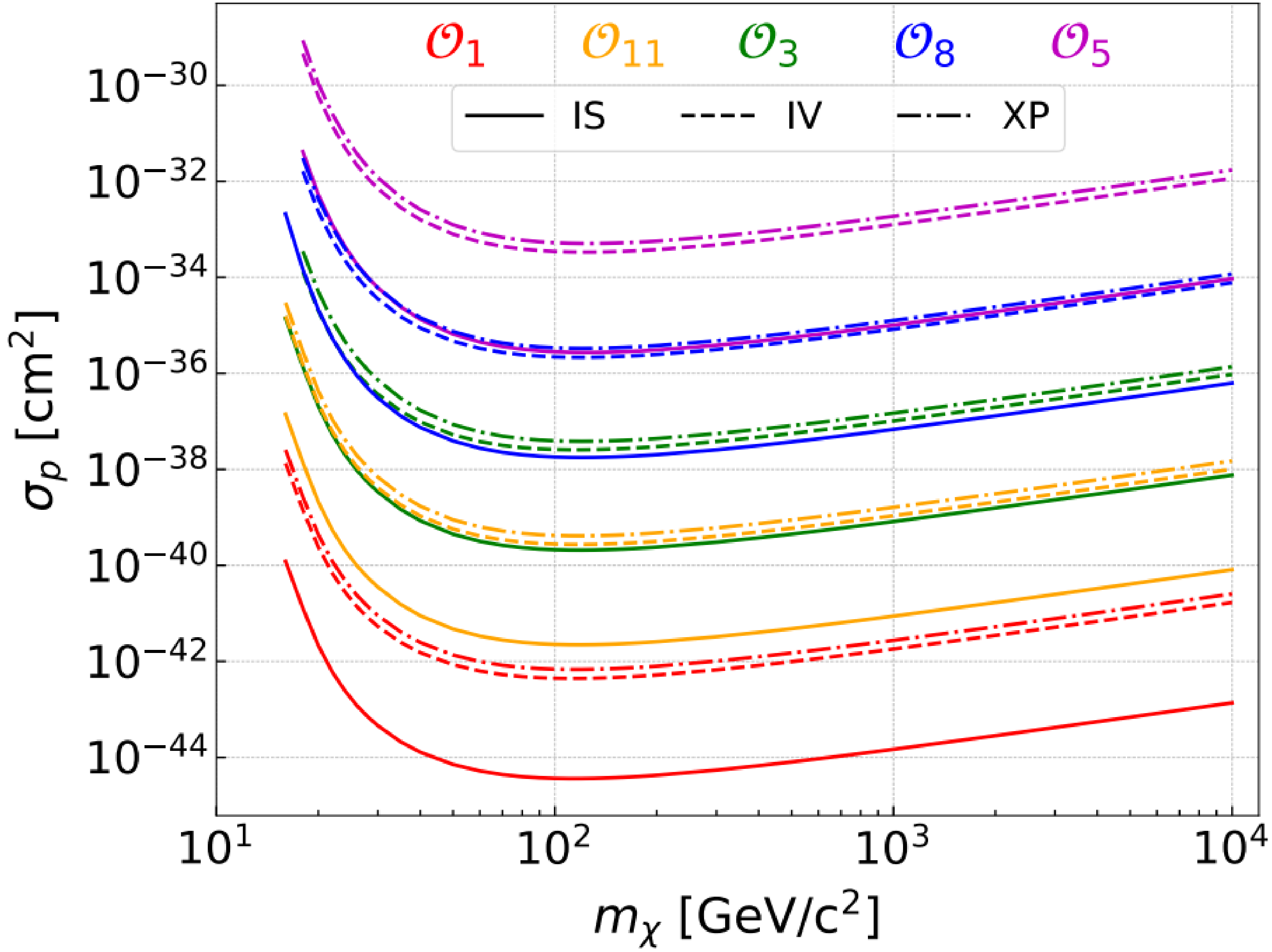

Effective DM-proton cross section

$$\sigma_p \equiv \frac{(c_i^p\,\mu_p)^2}{\pi}$$

Isoscalar **(IS)** -- $c_n/c_p = 1$

Isovector **(IV)** -- $c_n/c_p = -1$

Xenonphobic **(XP)** -- $c_n/c_p = -0.7$

Isospin-violating scenarios

Traditional SHM parameters used:

- Local DM density (ρ_0) : 0.3 GeV/cm^3
- Circular speed (v_0) : 220 km/s
- Escape speed (v_{esc}) : 544 km/s
- Velocity distribution : Maxwell-Boltzmann (boosted to the Earth reference frame).

Effects of substructures on O_1 and O_5

- Strongest effects at lower m_χ where the experiment probe the high-velocity tail of the distributions.
- Limits behave quite different at high-masses for O_5 due to its dependence with $v_\perp$ (enhancement/reduction in sensitivity). Non-linear effect, result of merging the astrophysical and particle physics uncertainties.

Phys.Rev.D 102 (2020) 8, 082001

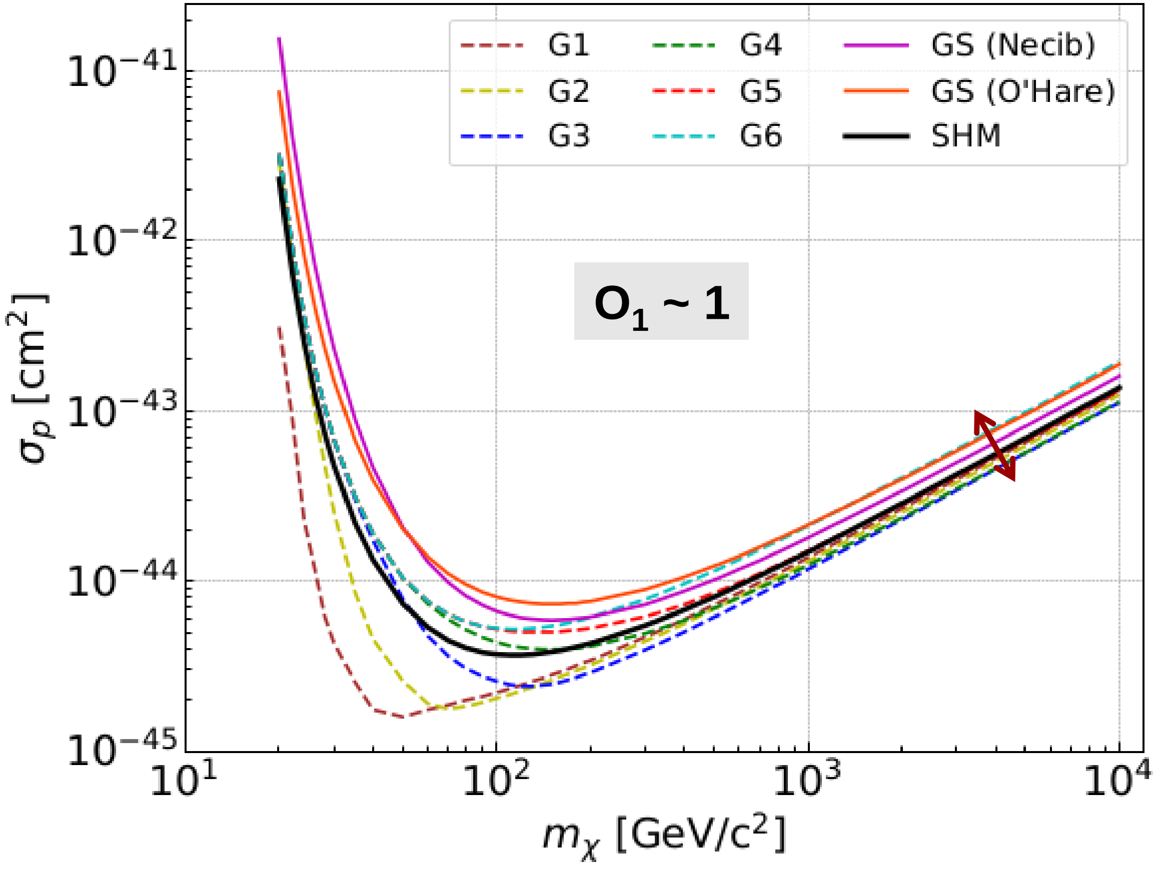

(a) $\mathcal{O}_1$ interactions

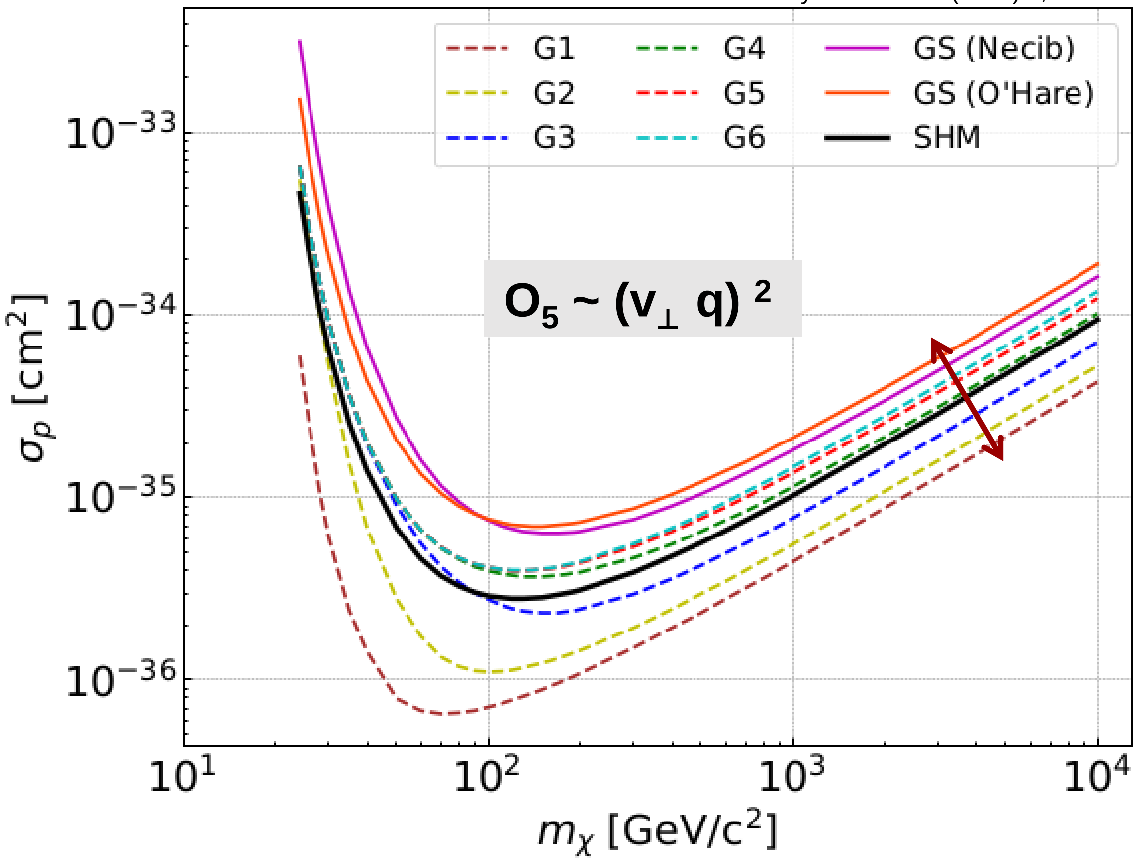

(b) $\mathcal{O}_5$ interactions

Exclusion limits showing the impact of substructures

Phys.Rev.D 102 (2020) 8, 082001

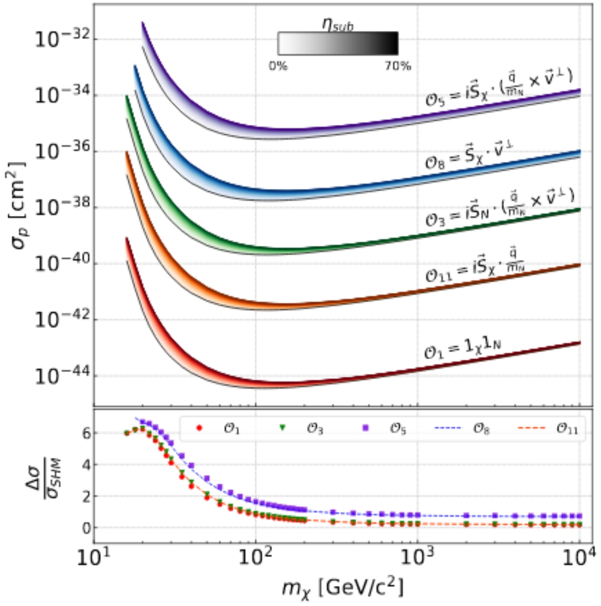

(a) *Gaia* Sausage (Necib *et al.*) [60]

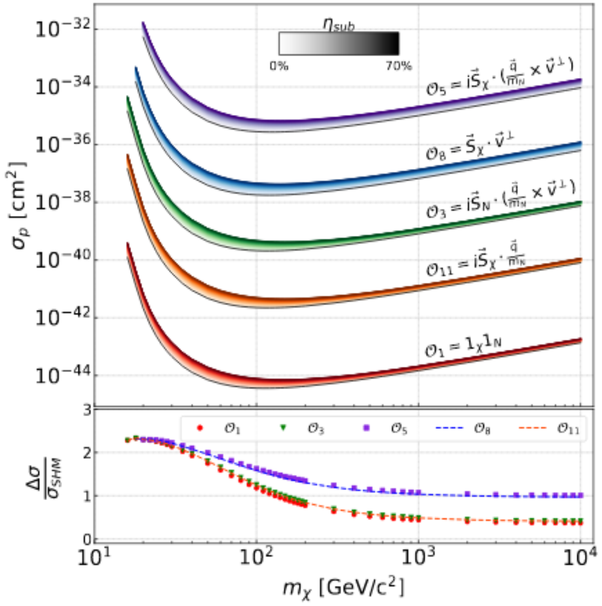

(b) *Gaia* Sausage (O'Hare *et al.*) [17]

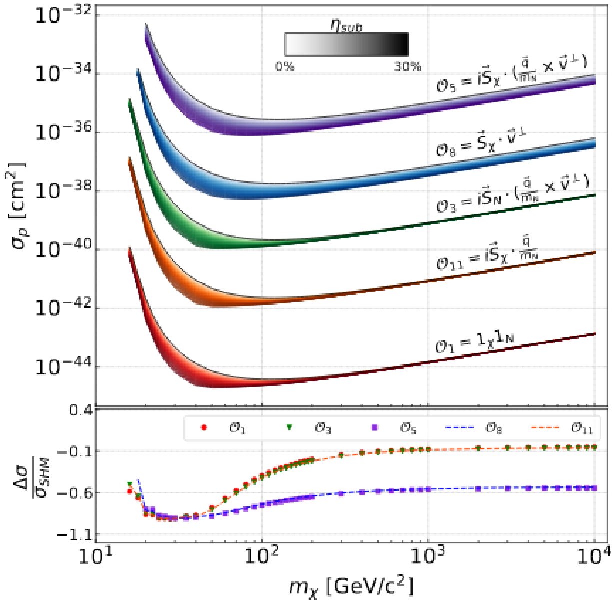

(c) G1 streams

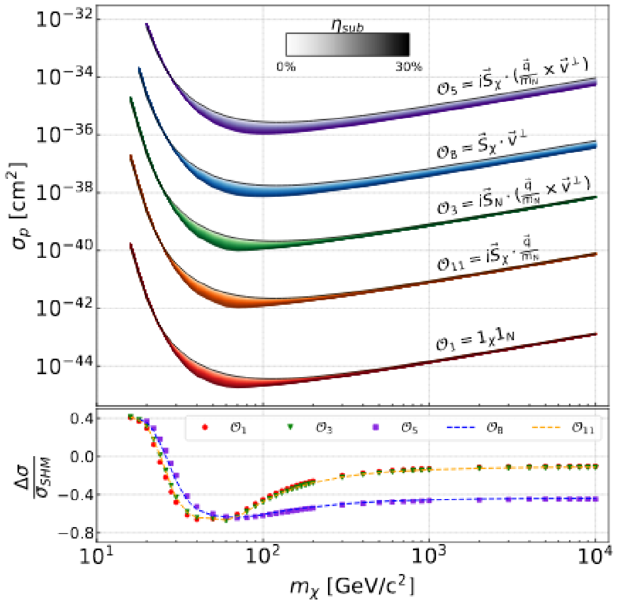

(d) G2 streams

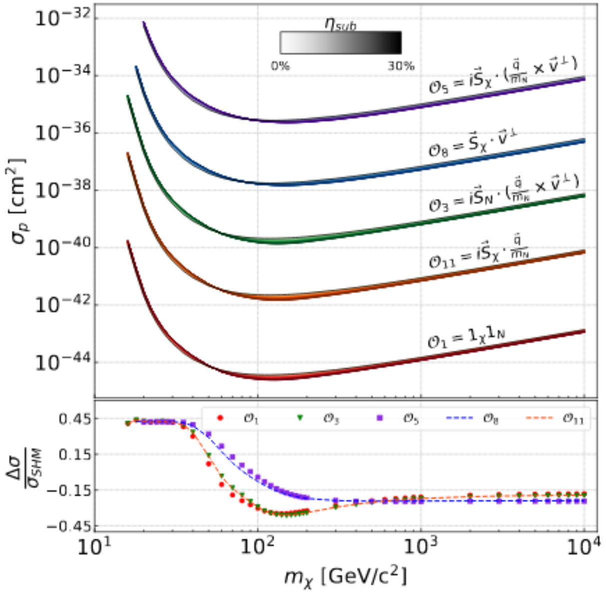

(a) G3 streams

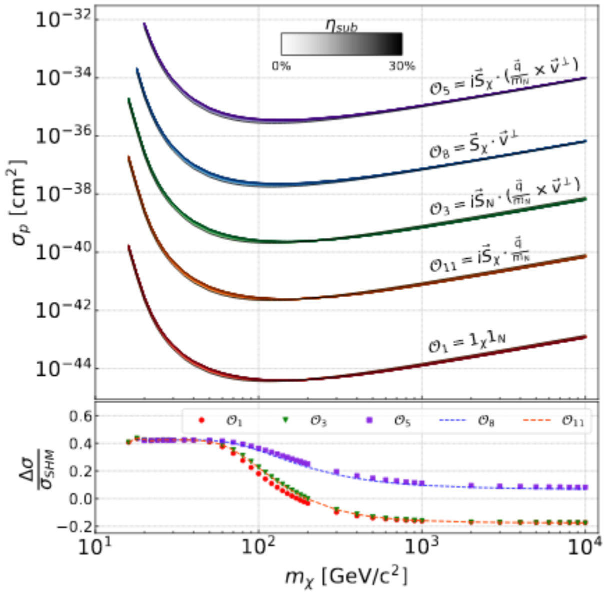

(b) G4 streams

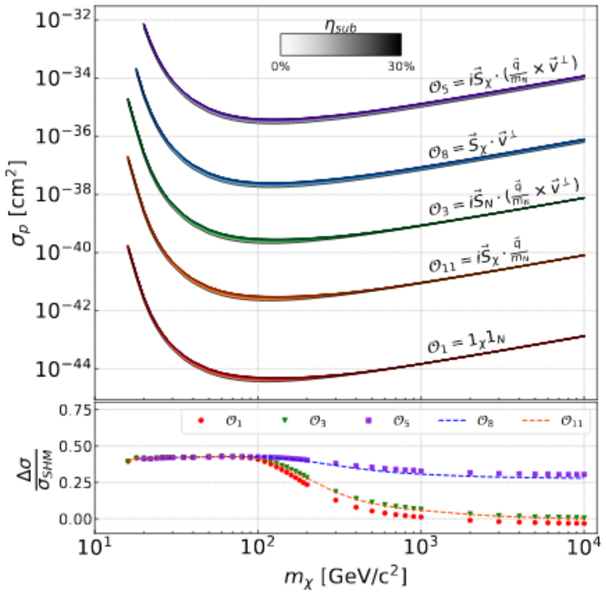

(c) G5 streams

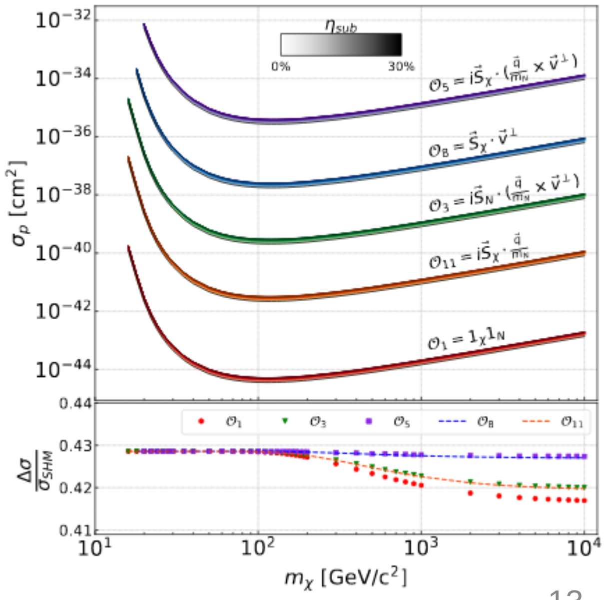

(d) G6 streams

Limits on specific interactions

Phys.Rev.D 102 (2020) 8, 082001

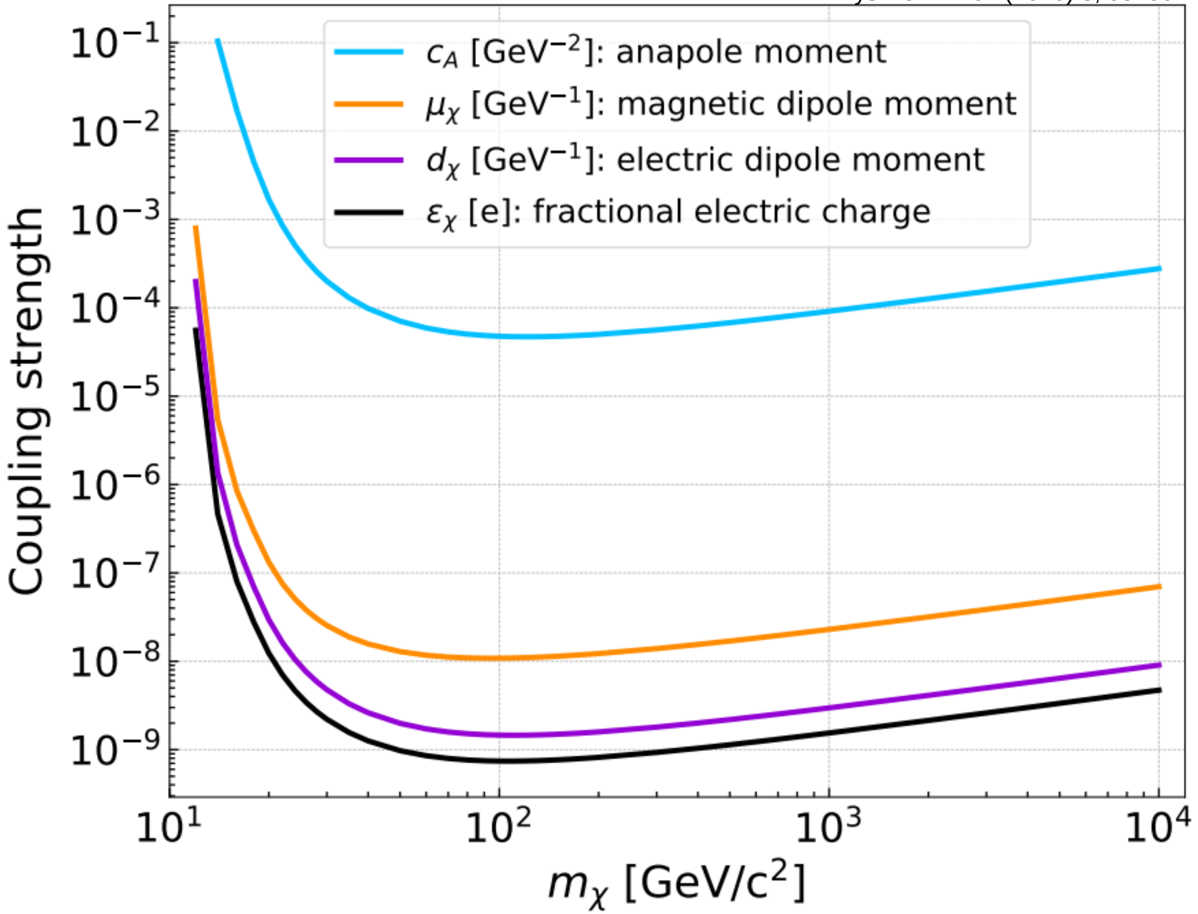

Limits on Xenonphobic Dark Matter

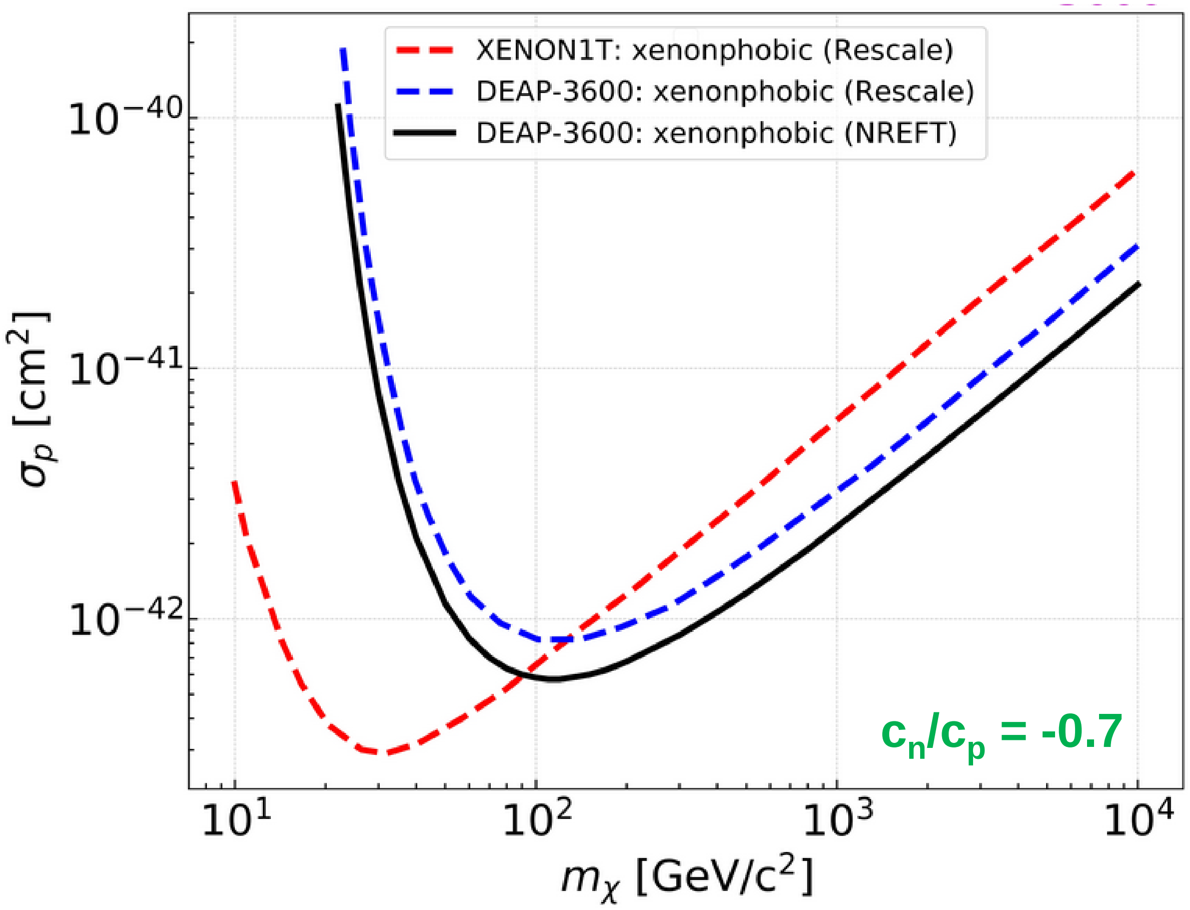

Final remarks

1. Reinterpreted the previous DEAP-3600 null result (231 live-days, 1st year of operation) with a NREFT framework and potential DM substructures in the local halo.

2. Constraints on effective contact operators O_1, O_3, O_5, O_8, O_{11}, isospin-violating cases (isovector, xenonphobic), and specific interactions (millicharge, magnetic dipole, electric dipole, anapole).

3. Studied the impact of halo substructures on the operators. $v_\perp$ -dependent operators (O_5,O_8) are particularly sensitive to the velocity distribution.

4. A nearly constant event rate for some scenarios might imply extending the ROI to higher energies, allowing some distinguishing information in the recoil spectrum shape if we have a future detection.

5. We achieved leading sensitivity for isospin-violating DM in the "Xenonphobic" regime. In case of any detection the complementarity between multiple targets is needed.

6. The astrophysical and particle physics uncertainties can significantly affect how we constrain the parameter space.

Full set of exclusion curves for all model combinations available online:

- Zenodo (DOI: 10.5281/zenodo.3998892): https://zenodo.org/record/3998892
- GitHub: https://github.com/arzure89/DEAP3600_arXiv-2005.14667/tree/v1.0

Thanks for your attention

Extra slide: Argon Pulse-Shape Discrimination

DEAP Collaboration. Eur. Phys. J. C 80, 303 (2020)
arXiv:2103.12202v2

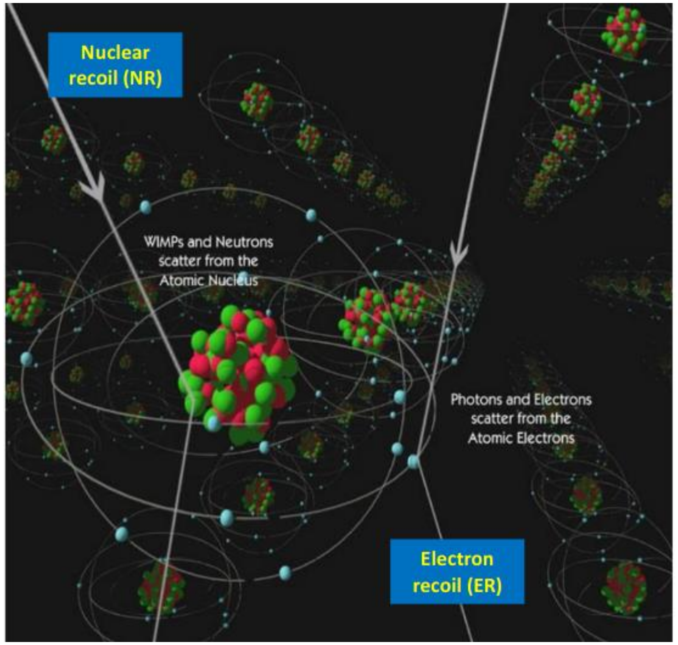

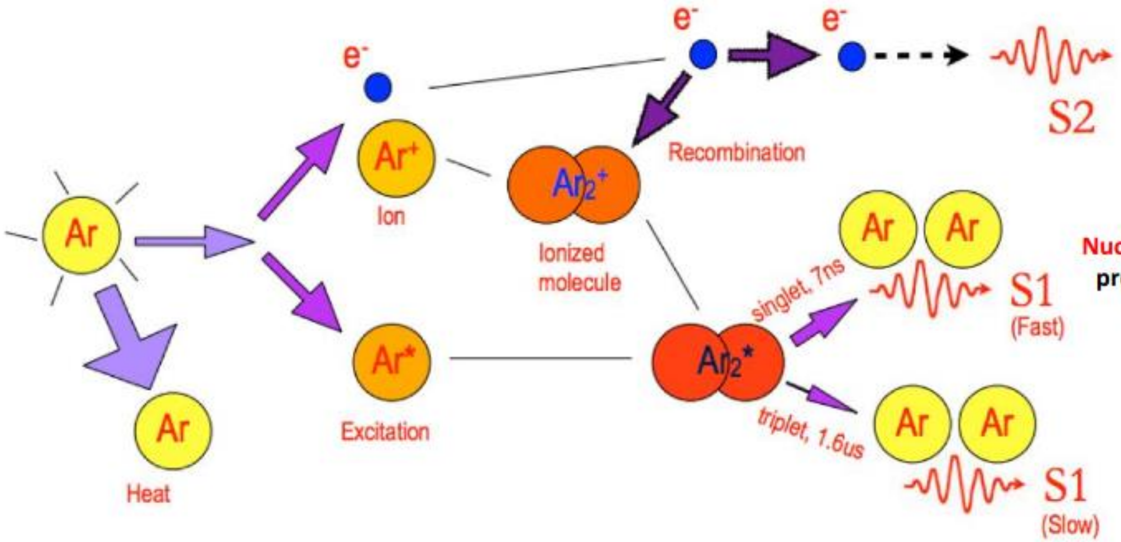

Nuclear recoils excite predominantly the singlet state

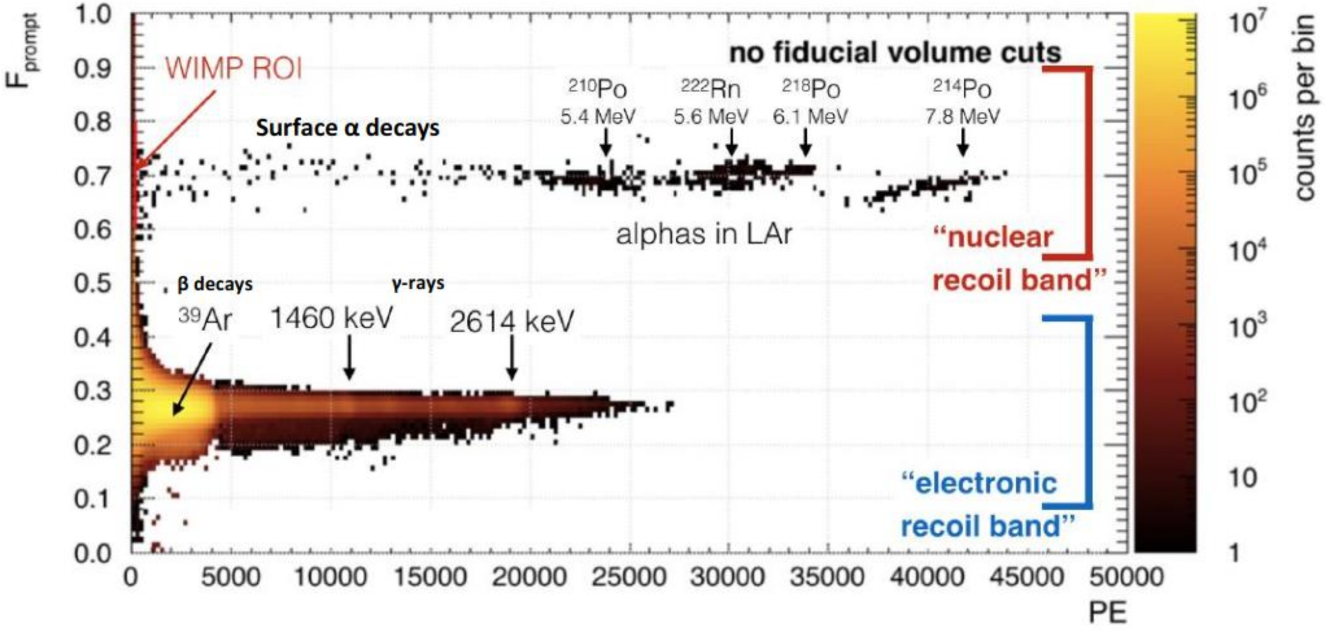

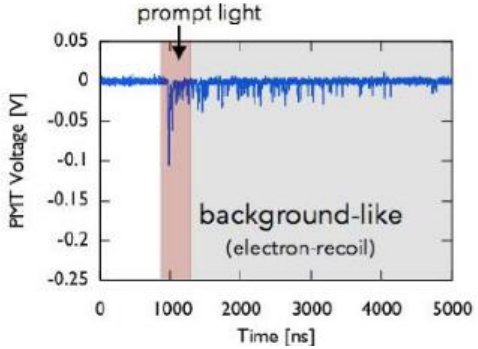

signal events have more prompt light!

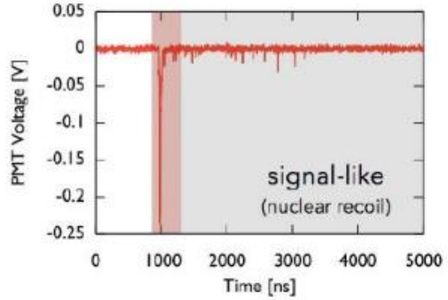

$$F_{prompt} = \frac{\text{Prompt PE } [-28, 60] \text{ ns}}{\text{Total PE } [-28, 10\,000] \text{ ns}}$$

Extra slide: Backgrounds in DEAP-3600

LAr: Ar39 β decays, α decays from Rn222/ Rn220,

Acrylic Vessel (AV) surface: Po210 α decays.

PMTs & other detector components: Radiogenic neutrons, γ/β produced in glass…

➡ Cherenkov light produced in light guide acrylic.

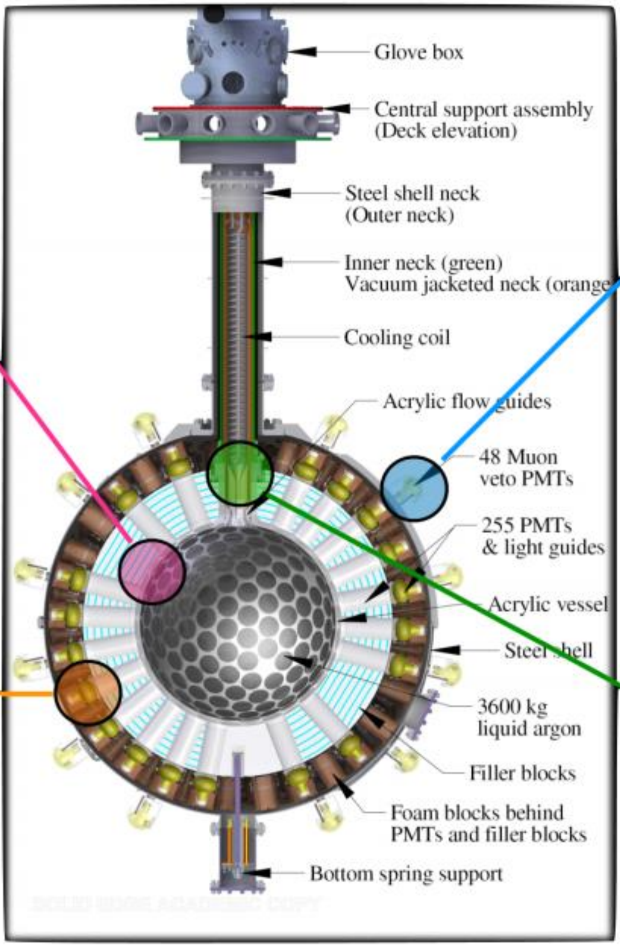

External: Cosmogenic-induced neutrons produced inside water tank/ rock.

Neck: Po210 α decays through LAr 'film' on surface of acrylic flowguides, originating from long-lived Pb210 (Rn222).

Phys. Rev. D 100, 022004 (2019)

	Source	N^{CR}	$N^{ROI,\ LL}$	N^{ROI}
β/γ's	ERs	2.44×10^9	0.34 ± 0.11	0.03 ± 0.01
	Cherenkov	$< 3.3 \times 10^5$	< 3890	< 0.14
n's	Radiogenic	6 ± 4	11^{+8}_{-9}	$0.10^{+0.10}_{-0.09}$
	Cosmogenic	<0.2	<0.2	<0.11
α's	AV surface	<3600	< 3000	< 0.08
	AV Neck FG	28^{+13}_{-10}	28^{+13}_{-10}	$0.49^{+0.27}_{-0.26}$
	Total	N/A	< 4910	$0.62^{+0.31}_{-0.28}$